Journal of Hazardous Materials 250–251 (2013) 345–353

Contents lists available at SciVerse ScienceDirect

Journal of Hazardous Materials

journal homepage: www.elsevier.com/locate/jhazmat

# Fe(II)–Al(III) layered double hydroxides prepared by ultrasound-assisted co-precipitation method for the reduction of bromate

Yu Zhong[a,b], Qi Yang[a,b,*], Kun Luo[a,b], Xiuqiong Wu[a,b], Xiaoming Li[a,b,*], Yang Liu[a,c], Wangwang Tang[a,b], Guangming Zeng[a,b], Bo Peng[a,b]

[a] College of Environmental Science and Engineering, Hunan University, Changsha 410082, China
[b] Key Laboratory of Environmental Biology and Pollution Control, Hunan University, Ministry of Education, Changsha 410082, China
[c] Urban and Rural Garbage Disposal Technology Research Center, Hunan Province, Changsha 410082, China

## HIGHLIGHTS

- Fe(II)–Al(III) LDHs were synthesized by ultrasound-assisted co-precipitation method.
- The Fe–Al (30 min) exhibited highly reduction reactivity on bromate.
- Pseudo-first-order model described the experimental data well.
- The mechanisms of bromate removal were proposed.

## GRAPHICAL ABSTRACT

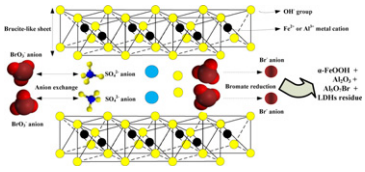


## ARTICLE INFO

*Article history:*
Received 4 November 2012
Received in revised form 3 January 2013
Accepted 29 January 2013
Available online xxx

*Keywords:*
Bromate
Fe(II)–Al(III) layered double hydroxides (Fe–Al LDHs)
Reduction
Ultrasound-assisted co-precipitation

## ABSTRACT

Bromate is recognized as an oxyhalide disinfection byproduct in drinking water. In this paper, Fe(II)–Al(III) layered double hydroxides (Fe–Al LDHs) prepared by the ultrasound-assisted co-precipitation method were used for the reduction of bromate in solution. The Fe–Al LDHs particles were characterized by X-ray diffractometer, scanning electron microscopy and thermogravimetry–differential scanning calorimetry. It was found that ultrasound irradiation assistance promoted the formation of the hydrotalcite-like phase and then improved the removal efficiency of bromate. In addition, the effects of solid-to-solution ratio, contact time, initial bromate concentration, initial pH, coexisting anions on the bromate removal were investigated. The results showed the bromate with an initial concentration of 1.56 μmol/L could be completely removed from solution by Fe–Al LDHs within 120 min. When the initial bromate concentration was 7.81 μmol/L, the Fe–Al LDHs with irradiation time of 30 min exhibited the optimum removal efficiency and the bromate removal capacity ($q_e$) was 6.80 μmol/g. In addition, the appearance of sulfate and production of bromide were observed simultaneously in this process, which suggested that ion-exchange between sulfate and bromate, and the reduction of bromate to bromide by $Fe^{2+}$ were the main mechanisms responsible for the bromate removal by Fe–Al LDHs.



## 1. Introduction

Bromate ($BrO_3^-$) is an oxyhalid disinfection byproduct (DBP) during chlorination or ozonation in bromide-containing water treatment [1,2], which has been found at the concentration as high as 150 μg/L following ozonation and advanced oxidation of drinking water [3]. Currently, bromate is regarded as a possible carcinogen [4] and has been confirmed to cause renal cell tumors in rats with the addition of potassium bromate into drinking water [5,6]. The International Agency for Research on Cancer (IARC) has classified it as a group B-2 carcinogen (as a possible human carcinogen) [7]. Consequently, the enforceable maximum contaminant level (MCL) of bromate in drinking water has been established at 10 μg/L (0.078 μmol/L) in the European Union, America and China [8]. Thus, it is necessary to develop

* Corresponding authors at: College of Environmental Science and Engineering, Hunan University, Changsha 410082, China. Tel.: +86 731 88822829; fax: +86 731 88822829.
*E-mail addresses:* yangqi@hnu.edu.cn, yangqi0622@yahoo.com.cn (Q. Yang), xmli@hnu.edu.cn (X. Li).

0304-3894/$ – see front matter © 2013 Elsevier B.V. All rights reserved.
http://dx.doi.org/10.1016/j.jhazmat.2013.01.081

some effective methods to control or removal bromate in drinking water.

Due to the high solubility, stability and non-biodegradation in water, bromate is difficult to eliminate once it is formed. The majority of researches have concentrated on optimizing ozonation processes to mitigate bromate formation. Chlorine or ammonia are usually used to control bromate formation during ozonation [9,10]. For another, a wide range of techniques by several chemical, physical and biological methods have also been investigated to decrease bromate after its formation. Several adsorbents such as activated carbon [11,12], nano crystalline akaganeite (β-FeOOH)-coated quartz sand (CACQS) [8], ion exchange membrane bioreactors [13] have shown the abilities to adsorb bromate from aqueous solutions. Meanwhile, the reduction of bromate to innocuous bromide has been achieved by activated carbon felt electrodes [14], zero-valent iron [15], granular ferric hydroxide [16], $Pd/Al_2O_3$ catalysts [17], and biological reduction [18].

Recently, layered double hydroxides (LDHs) have been received more attention as anion-exchange materials for the adsorption of bromate from aqueous solutions [19], owing to their large surface area, high anion exchange capacity and excellent thermal stability [19,20]. In fact, LDHs materials have been also investigated as reducing agent. For example, Hansen et al. [21] studied the reduction of nitrite or nitrate into ammonium ion by Fe(II)–Fe(III) LDHs. In most literatures, conventional co-precipitation is the main method to prepare LDHs, which will produce unstable large LDHs particles and require longer aging time [22,23]. Many literatures have shown that ultrasound has a positive effect on nucleation by shifting the size distribution toward small particles and modifying the morphology [24]. Chang et al. [25] found that the ultrasound irradiation induced the production of high crystalline calcined LDH with relatively small particle size, large specific surface area, high adsorption ability for fluoride, and a requirement of short aging time. Therefore, it is of high interest to quantitatively assess whether ultrasound has a positive effect on primary nucleation, and Fe–Al LDHs reactivity to bromate reduction.

Fe(II)–Al(III) LDHs, as an adsorbing/reducing agent, were successfully prepared through co-precipitation under the assistance of ultrasound irradiation in this study. The main objectives of this paper were (i) to investigate the optimal ultrasound irradiation time to prepare the Fe–Al LDHs, (ii) to evaluate the effect of solid-to-solution ratio, contact time, initial bromate concentration, initial pH and coexisting anions on bromate removal by batch experiments, and (iii) to explain the possible mechanisms involved in the removal of bromate by Fe–Al LDHs.

## 2. Materials and methods

### 2.1. Chemicals

All the chemical reagents used in this work were of analytical grade. Milli-Q ultrapure water (18.2 MΩcm) was used throughout the study and adequately purged with $N_2$ before use. $FeSO_4{\bullet}7H_2O$ (assay 99%), $Al_2(SO_4)_3{\bullet}18H_2O$ (assay 99%), NaOH (assay 96%) and $H_2SO_4$ (assay 98%) were purchased from Kermel Chemical Reagent Co. Ltd. (Tianjin, China). Stock solution of bromide ($Br^-$) and bromate ($BrO_3^-$) was prepared by dissolving certain amount of NaBr (assay 99%) and $NaBrO_3$ (assay 99.7%) in ultrapure water, respectively.

### 2.2. Synthesis of Fe–Al LDHs

The Fe–Al LDHs were synthesized by an ultrasound-assisted co-precipitation method with nitrogen gas bubbling. Solution A was prepared by dissolving $FeSO_4{\bullet}7H_2O$ (5.6 g, 0.02 mol $Fe^{2+}$) and $Al_2(SO_4)_3{\bullet}18H_2O$ (3.3 g, 0.01 mol $Al^{3+}$) in 200 mL ultrapure water, and solution B was prepared by dissolving NaOH (16.0 g, 0.4 mol $OH^-$) in 200 mL ultrapure water. Then, solution B was dripped into solution A in a 500 mL glass Erlenmeyer flask at a stirring rate of 800 rpm, and the pH of resulting suspension was maintained at 9.0 ± 0.5. The mixed solution was covered with a stopper and transferred immediately into an ultrasound generator (KQ-500E, Kunshan Ultrasound Instrument Co. Ltd.) operating at 80 kHz with a power of 160 W, and the temperature was kept at 65 °C. This procedure was carried out for different irradiation times: 15, 30, 60, and 90 min. These samples were labeled as Fe–Al (15 min), Fe–Al (30 min), Fe–Al (60 min), Fe–Al (90 min), respectively. The final products were separated by filtration, washed twice with 100 mL ultrapure water and dried in a vacuum at 90 °C for 24 h. The obtained samples were stored in tightly capped bottles for further use.

For comparison, Fe–Al LDHs was also synthesized by using the similar procedures with the aging time of 30 min but without ultrasound irradiation, the sample was labeled as Fe–Al (0 min).

### 2.3. Characterization

Samples were characterized by an X-ray diffractometer (Siemens D5000, Germany) with Cu Kα radiation (λ = 1.5406 Å) operating at 50 kV voltage and 30 mA current. Patterns of Fe–Al LDHs were recorded from 2° to 80° (in 2θ) with a 0.02° step width and a scanning rate of 2° $min^{-1}$.

The morphology of Fe–Al LDHs was performed by scanning electron microscopy (SEM) using a TM3000 microscope (Hitachi Limited, Japan). Thermal analysis experiments of the samples were carried out in a thermogravimetry–differential scanning calorimetry (TG–DSC) instrument (Netzsch STA-409PC/PG, Germany) with $N_2$ as carrier gas at a heating rate of 10 °C $min^{-1}$ up to 800 °C. Elemental analyses were performed by inductively coupled plasma (ICP) atomic emission spectrometry (Baird PS-6, USA).

### 2.4. Bromate removal experiments

Bromate removal experiments were performed using a batch experiment, which were carried out in 250 mL glass Erlenmeyer flask at room temperature unless otherwise stated. The concentrations of bromate ($BrO_3^-$) and bromide ($Br^-$) in solutions were analyzed using an ion chromatography (Dionex ICS-900, USA) equipped with a suppressed conductivity detector, and a 500 μL sample loop (detection limit = 0.0078 μmol/L). All the experiments were conducted in duplicate.

#### 2.4.1. Effect of solid-to-solution ratio

Fe–Al LDHs (0.05–0.4 g) were added to 200 mL bromate solution (1.56 μmol/L) at initial pH 7.0 with the contact time of 24 h.

#### 2.4.2. Effect of contact time

Fe–Al LDHs (0.2 g) were added in 200 mL bromate solution (1.56 μmol/L), and a small amount of the sample was sampled at intervals of 15, 30, 60, 120, 180, 240, and 1440 min, respectively.

#### 2.4.3. Effect of initial bromate concentration

Fe–Al LDHs (0.2 g) were mixed with 200 mL bromate solution (0.78–7.81 μmol/L) and were stirred for 24 h using a magnetic stirrer.

#### 2.4.4. Effect of initial pH

Fe–Al LDHs (0.2 g) were stirred in 200 mL bromate solution (1.56 μmol/L) for 24 h at pH in the range 2.0–11.0. The initial pH was adjusted by the addition of 1.0 mol/L $H_2SO_4$ or 1.0 mol/L NaOH.

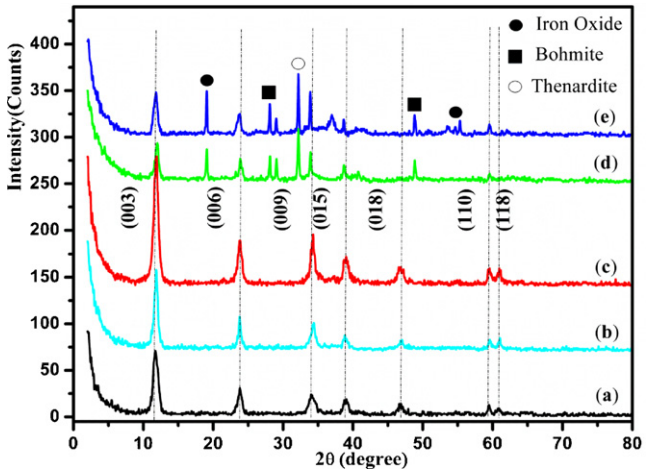


**Fig. 1.** XRD patterns of Fe–Al LDHs prepared at different irradiation times. (a) Fe–Al (0 min), (b) Fe–Al (15 min), (c) Fe–Al (30 min), (d) Fe–Al (60 min), and (e) Fe–Al (90 min).

### 2.5. Calculations

The removal capacity of bromate was calculated as follows:

$$q_e = (C_0 - C_t) \times \frac{V}{m} \quad (1)$$

where $q_e$ (μmol/g) is the bromate removal capacity of Fe–Al LDHs at time $t$, $V$(L) is the volume of solution, $C_0$ (μmol/L) and $C_t$ (μmol/L) are initial bromate concentration and bromate concentration at time $t$, respectively; and $m$ (g) is the mass of Fe–Al LDHs.

## 3. Results and discussion

### 3.1. Characterization

#### 3.1.1. X-ray diffraction

XRD patterns of the Fe–Al LDHs prepared at different irradiation times were presented in Fig. 1. It was observed that the Fe–Al (0 min), Fe–Al (15 min), and Fe–Al (30 min) exhibited symmetric reflections of the basal (0 0 3) and (0 0 6) planes, which were the characterization of typical layered structure [26]. Compare with the Fe–Al (0 min) samples, the ultrasound assistance with appropriate time (15–30 min) produced slightly higher intensity and sharper peaks. With the irradiation time increased from 15 min to 30 min, the characteristic peaks (0 0 3) and (0 0 6) of hydrotalcites increased, indicating that the application of ultrasound in the preparation process promotes the formation of the hydrotalcite-like phase [25]. The distinct reflections observed for the Fe–Al LDHs were (0 0 3), (0 0 6), (0 0 9), (0 1 5), and (1 1 0) indexed with a rhombohedral symmetry (3R) stacking sequence [27]. The composition of the sample with a LDH structure could be estimated by fitting the elemental analysis of cations, anions, and water molecules in the general formula of the LDH $[M^{2+}_{1-x}M^{3+}_{x}(OH)_2]^{x+}(A_{x/n})^{n-}mH_2O$ [28], The Fe–Al (30 min) composition was estimated as $[Fe_{0.671}Al_{0.329}(OH)_2][(SO_4)_{0.164}\bullet 1.11\ H_2O]$ with the Fe/Al molar ratio of approximately 2/1, which was consistent with the ratio in the starting solution.

In contrast, Fe–Al (60 min) and Fe–Al (90 min) exhibited no significant LDHs structure with characteristic peaks (0 0 3) and (0 0 6) of hydrotalcites decreased. As evidenced from XRD patterns, the products were the mixture of bomhite (JCPDS Card 21-1307), thenardite (JCPDS Card 70-1541), and iron oxide (JCPDS Card 26-1136), indicating that when the irradiation time is too long, a great amount of $Fe^{2+}$ was oxidized to $Fe^{3+}$. Walton et al. [29] also reported that the ultrasound irradiation promoted the electrochemical oxidation of ferrous ions to ferric ions, which could be explained with "acoustic cavitation" [30]. The dried LDHs material of Fe–Al (0 min), Fe–Al (15 min), and Fe–Al (30 min) were dark green, but the color of Fe–Al (60 min) and Fe–Al (90 min) were red brown, which also illustrated a tendency of oxidation of $Fe^{2+}$ to $Fe^{3+}$ [31].

#### 3.1.2. Scanning electron microscopy

SEM was employed to understand the morphology evolution process of Fe–Al LDHs prepared at different ultrasound irradiation times. Fig. 2a showed that Fe–Al (0 min) presented a large number of oblique polyhedron particles with an average size of 1.0–1.5 μm. The Fe–Al (15 min) consisted of well dispersed microspheres with the particle size of 0.5–1.0 μm (Fig. 2b). With the irradiation time increased to 30 min, most of the nanoparticles were about 0.1–0.5 μm (Fig. 2c). Thus, Fe–Al (15 min) and Fe–Al (30 min) produced more nanoparticles than the Fe–Al (0 min), indicating that the ultrasound during the aging process contributed to the decrease of the particle sizes, which was consistent with the results of the XRD analysis.

When the irradiation time increased to 60 min, the microspheres still existed in the form of hierarchical nanoparticles, but the size increased to 1–5 μm (Fig. 2d). With the increase of the irradiation time to 90 min, uniform flowerlike hierarchical porous structures emerged, thus no nanoparticles remained and the sample consisted entirely of flowerlike hierarchical microspheres assembled with nanoparticles, which were about 4–8 μm in width (Fig. 2e). It seemed that flowerlike hierarchical microspheres were self-assembled by the secondary LDHs nanoparticles with about 0.5 μm in length, and were also formed by 1–8 μm sized primary particles. It was similar to the observation reported by Abbasi et al. [32] that the average particle size in the solution considerably increased when the reaction time was prolonged to 120 min.

#### 3.1.3. Thermal gravimetric analysis

The TG–DSC curves of the synthesized samples were presented in Fig. 1S (see Supporting information). Fe–Al (0 min), Fe–Al (15 min), and Fe–Al (30 min) showed three endothermic peaks in their DSC curves that were typical peaks of the LDHs materials [33,34]. The first drop (20–200 °C) was due to the removal of weakly adsorbed and interlayer water molecules with endothermic peaks around 143 °C. The second drop (200–400 °C) was mainly caused by the dehydroxylation of the brucite-like layers [35]. The third drop (400–800 °C) was attributed to the decomposition of sulfate anion under nitrogen gas in the LDHs [35,36]. According to the TG analysis, the total weight loss was 31.81%, 21.77%, and 23.83% for Fe–Al (0 min), Fe–Al (15 min), and Fe–Al (30 min) during the thermal decomposition process, respectively.

The TG–DSC curves for Fe–Al (60 min) and Fe–Al (90 min) showed similar endothermic peaks between 20 and 400 °C. The first drop was due to the removal of physically adsorbed water, the second drop was caused by the removal of chemisorbed water, and the third drop between 400 and 700 °C with a significant weight loss was ascribed to the decomposition of sulfate anion and the formed water [37]. The total weight loss for Fe–Al (60 min) and Fe–Al (90 min) was 25.30% and 26.37%, respectively.

### 3.2. Bromate removal by Fe–Al LDHs

#### 3.2.1. Effect of solid-to-solution ratio

The ability of bromate removed by Fe–Al LDHs was examined by varying the masses of the samples. Results of the residual bromate concentration in solutions against the amount of samples were depicted in Fig. 3. It was observed that the residual concentration of bromate in solutions decreased rapidly when the solid-to-solution ratio was up to 1.0 g/L. With the further increase of the

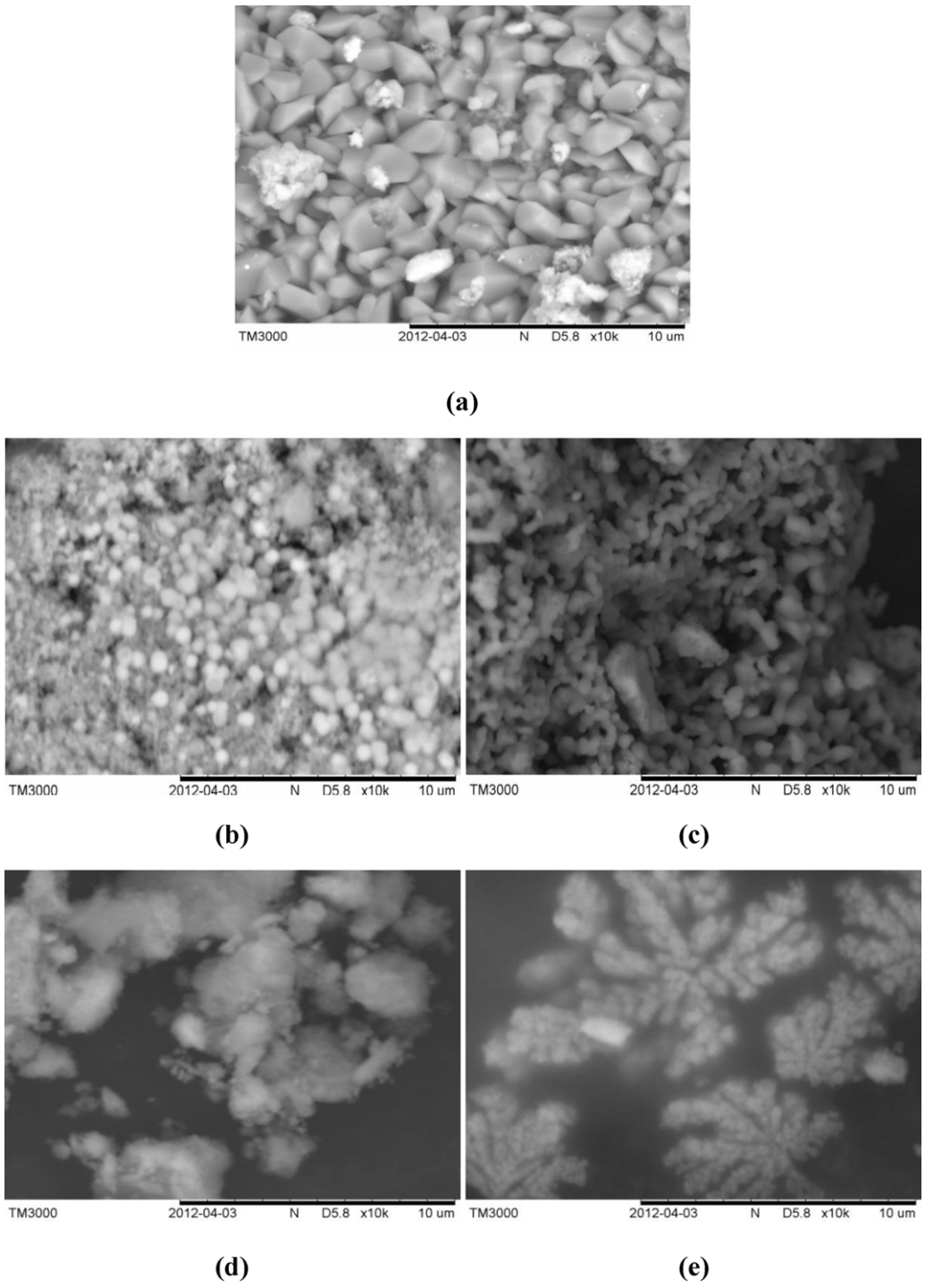


**Fig. 2.** SEM images of Fe–Al LDHs prepared at different irradiation times. (a) Fe–Al (0 min), (b) Fe–Al (15 min), (c) Fe–Al (30 min), (d) Fe–Al (60 min), and (e) Fe–Al (90 min).

solid-to-solution ratio to 2.0 g/L, the concentration of residual bromate in solutions remained almost constant. In previous literature, it had been proved that the structural $Fe^{2+}$ of the Fe–Al LDHs played an important role on the bromate reduction [21]. In addition, the increasing amount of the Fe–Al LDHs could enhance the removal efficiency of bromate because of the availability of more reactive sites. According to the surface site heterogeneity model, the surface is composed of sites with a spectrum of binding energies [38]. Therefore, the active reaction sites tend to exist at a fixed solution concentration. Consequently, a solid-to-solution ratio of 1.0 g/L was sufficient for the quantitative reduction of bromate, at which ratio the Fe–Al (15 min) and Fe–Al (30 min) all exhibited a slightly higher removal efficiency to bromate compared with Fe–Al (0 min), the $q_e$ for Fe–Al (0 min), Fe–Al (15 min), and Fe–Al (30 min) were 1.43 μmol/g, 1.56 μmol/g, and 1.56 μmol/g, respectively.

### 3.2.2. *Effects of contact time*

The effect of contact time on bromate removal by Fe–Al LDHs was presented in Fig. 4. Bromate, with the initial concentration of 1.56 μmol/L, could be decreased to lower than the maximum contaminant level (MCL) of 0.078 μmol/L by Fe–Al (15 min) and Fe–Al (30 min) within 120 min, indicating nearly 100% bromate

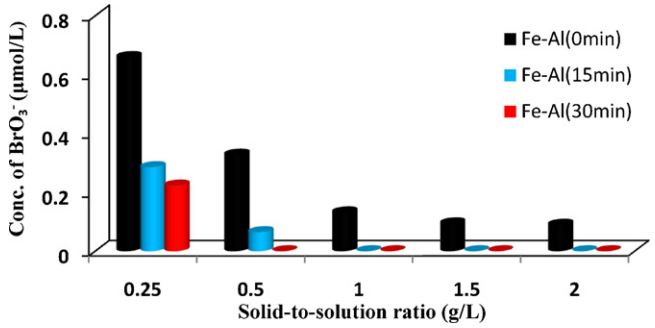


**Fig. 3.** Effect of solid-to-solution ratio on bromate removal by Fe–Al LDHs. Initial conc. of $BrO_3^-$ = 1.56 μmol/L, sample = 0.05–0.4 g, vol. = 200 mL, contact time = 24 h and initial pH = 7.0.

removal. However, the concentration of bromate in the Fe–Al (0 min) solution was still very high (ca. 0.13 μmol/L) after 1440 min. The removal efficiency of bromate after 120 min was 64.4%, 100%, and 100% for Fe–Al (0 min), Fe–Al (15 min), and Fe–Al (30 min), respectively. The higher removal efficiency of Fe–Al (15 min) and Fe–Al (30 min) indicated clearly that the removal of bromate could be highly enhanced by the ultrasonic irradiation during the preparation of the Fe–Al LDHs.

### 3.2.3. Effect of initial bromate concentration

The effect of initial bromate concentration (0.78–7.81 μmol/L) on the bromate removal by Fe–Al LDHs was illustrated in Fig. 5. When the initial bromate concentration varied from 0.78 to 7.81 μmol/L, the $q_e$ dramatically increased from 0.76 to 6.08 μmol/g, 0.78 to 6.66 μmol/g, and 0.78 to 6.80 μmol/g for Fe–Al (0 min), Fe–Al (15 min), and Fe–Al (30 min), respectively. However, it was noticed that with the initial bromate concentration over 1.56 μmol/L, the residual bromate for Fe–Al (0 min) was higher than the enforceable MCL of 0.078 μmol/L, but those for Fe–Al (15 min) and Fe–Al (30 min) were lower than the level until the initial bromate concentration was up to 4.68 μmol/L, which suggested that the application of ultrasound in the preparation process was conducive to improve the bromate removal capacity by Fe–Al LDHs. The ultrasound prepared Fe–Al LDHs showed higher bromate removal capacity than other adsorbents. In previous literatures, the bromate removal capacity by coal-based carbon was only 3.51 μmol/g [39]. Chitrakar et al. [19] found that calcined Mg-Al LDHs was also effective for decreasing bromate and the bromate adsorption capacity was 0.70 μmol/g.

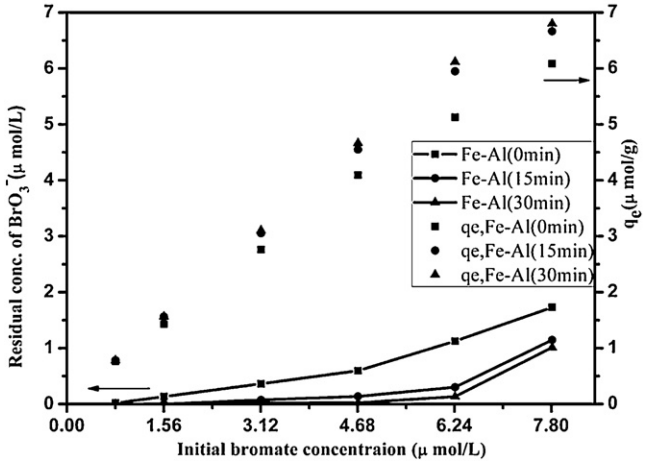


**Fig. 5.** Effect of initial bromate concentration on bromate removal by Fe–Al LDHs. Sample = 0.2 g, vol. = 200 mL, contact time = 24 h and initial pH = 7.0.

### 3.2.4. Effect of initial pH

The effect of pH on bromate removal by Fe–Al LDHs was evaluated at initial pH 2.0–11.0 (Fig. 6). Data showed that complete removal of bromate occurred and the concentration of bromide was nearly equal to the initial concentration of bromate over the pH range of 7.0–11.0, which indicated that the Fe–Al LDHs had high ability to reduce bromate to bromide. It was noteworthy that Fe–Al LDHs displayed lower bromate removal at the acidic condition (pH 2.0–4.0). There were two reasons involved: Firstly, metal–metal–hydroxysalts began to dissolve and the metal cations in the LDHs layers at acidic condition were released into solution, which led to the decrease of bromate removal capacity [40]. Secondly, more sulfate ions turned up by adjusting initial pH of aqueous solution by $H_2SO_4$, which might inhibit the exchange of bromate with interlayer sulfate ions of LDHs. Kirisits et al. [41] found that the removal efficiency of bromate by biologically activated carbon (BAC) was better at lower pH values (6.8 and 7.2) than that at higher pH values (7.5 and 8.2). In addition, Wang et al. [15] reported that the reaction of zero-valent iron ($Fe^0$) with bromate was faster at pH 3.0 than that at pH 7.0–11.0, which might be that the iron oxide layer covering the $Fe^0$ core was dissolved more rapidly at pH 3.0, thus in turn accelerated the reaction of $Fe^0$ with bromate.

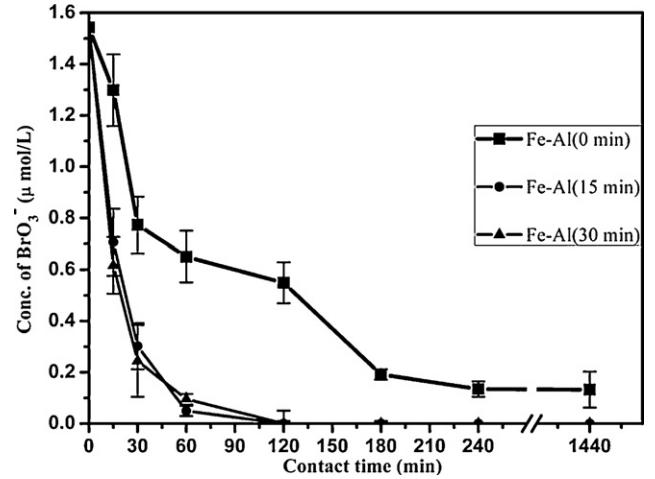


**Fig. 4.** Effect of contact time on bromate removal by Fe–Al LDHs. Initial conc. of $BrO_3^-$ = 1.56 μmol/L, sample = 0.2 g, vol. = 200 mL and initial pH = 7.0.

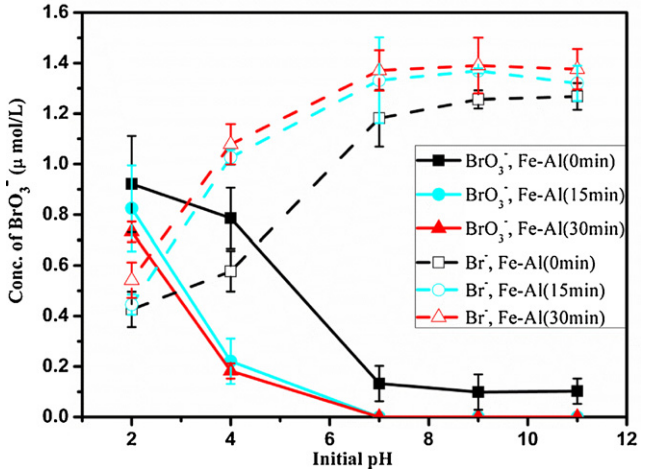


**Fig. 6.** Effect of initial pH on bromate removal by Fe–Al LDHs. Initial conc. of $BrO_3^-$ = 1.56 μmol/L, sample = 0.2 g, vol. = 200 mL and contact time = 24 h.

**Table 1**
Pseudo first-order rate constants of bromate removal by Fe–Al LDHs.

| Samples | $q_{e,measured}$ | $q_{e,calculated}$ | $k_1$ | $R^2$ |
|---|---|---|---|---|
| Fe–Al (0 min) | 4.0913 | 4.9629 | 0.0143 | 0.9629 |
| Fe–Al (15 min) | 4.5506 | 5.3888 | 0.0160 | 0.9725 |
| Fe–Al (30 min) | 4.6650 | 4.0068 | 0.0234 | 0.9582 |

### 3.3. Kinetics of bromate removal by Fe–Al LDHs

The kinetic studies of bromate removal by Fe–Al LDHs (0.2 g) were investigated at pH 7.0. The reaction kinetics could be described by the pseudo-first-order kinetic equation as:

$$\frac{dq}{dt} = k_1(q_e - q_t) \quad (2)$$

Its integrated form can be obtained as follows:

$$\ln(q_e - q_t) = \ln q_e - k_1 t \quad (3)$$

where $q_e$ and $q_t$ are the reaction loadings of bromate (μmol/g) on the removal at equilibrium and at time $t$ (min), respectively, $k_1$ is the pseudo-first-order reaction rate constant ($min^{-1}$) and $t$ is the contact time (min).

Table 1 gives the fitted model parameters. The higher correlation coefficient ($R^2$) varied from 0.9582 to 0.9725 suggested that the experimental data could be well described by the pseudo-first-order kinetic model. Karina et al. [42] also found that the dechlorination of carbon tetrachloride by Fe(II)–Fe(III) hydroxide followed the pseudo-first-order kinetic model. The average values of $k_1$ for Fe–Al (0 min), Fe–Al (15 min), and Fe–Al (30 min) was found to be 0.0143, 0.0160, and 0.0234 $min^{-1}$, respectively, which indicated that the reaction rates of Fe–Al (15 min) and Fe–Al (30 min) was 1.14 and 1.64 times that of Fe–Al (0 min), respectively.

### 3.4. Mechanism of bromate removal by Fe–Al LDHs

To explain the mechanism of bromate removal by Fe–Al LDHs, the concentration of bromide, bromate and sulfate were monitored simultaneously as a function of time ($C_t$) and the solution pH was not controlled during the reaction. Since the trend of the curve was similar, Fe–Al (30 min) was selected as an example to elucidate the reaction mechanism. In the initial 15 min, the removal of bromate by the Fe–Al LDHs was accompanied with the rapid increase of sulfate concentration in solution (Fig. 7b), which suggested that primary mechanism was ion-exchange adsorption at this stage. Meanwhile, the initial bromate concentration decreased from 4.69 to 3.43 μmol/L, and the bromide concentration increased from 0 to 0.06 μmol/L (Fig. 7a), thus the total concentration of bromate and bromide in the solution was ca. 3.49 μmol/L, which was far less than the initial concentration of bromate. It further suggested that the exchange of anion with sulfate in the interlayer region led to partial adsorption of bromate.

As time elapsed from 30 to 240 min, reduction reaction played a major role. Bromate obtained electrons from ferrous ions, and the concentration of bromide proportionally increased as the bromate concentration decreased from 2.52 μmol/L at 30 min to 0.02 μmol/L at 240 min. Correspondingly, the bromide concentration increased from 1.91 to 4.59 μmol/L (Fig. 7a), which was nearly equal to the initial bromate concentration, and the slight difference (0.10 μmol/L) should be attributed to the adsorption of a little bromide onto the interlayer region of LDHs. The phenomenon was consistent with the bromate reduction using zero-valent iron that bromate was reduced completely to bromide without the formation of intermediate product [43]. To further confirm this phenomenon, the XRD spectra of Fe–Al (30 min) after reaction with bromate were analyzed (Fig. 8). The amorphous domain could be seen among

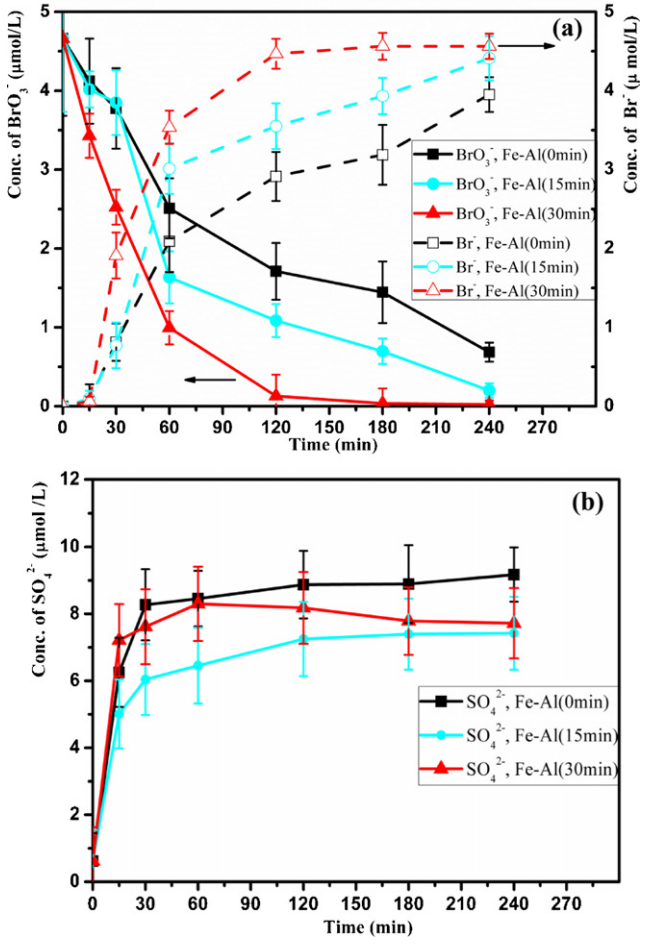


**Fig. 7.** (a) Bromate and bromide concentration during the bromate removal by Fe–Al LDHs. (b) Release of sulfate into solution on Fe–Al LDHs. Initial conc. of $BrO_3^-$ = 4.69 μmol/L, sample = 0.2 g, vol. = 200 mL and initial pH = 7.0.

the peaks for a mixture of poorly crystalline goethite (α-FeOOH), aluminum oxide bromide ($Al_5O_7Br$), aluminum oxide ($Al_2O_3$) and LDHs residue, and no additional bromate reduction products were observed. The layered structure of Fe–Al (30 min) collapsed completely due to the oxidation of $Fe^{2+}$ to $Fe^{3+}$ in the brucite-like layers. Chitrakar et al. [35] prepared Fe–Al LDH ($SO_4$ type) by co-precipitation method to reduce bromate. They found that the LDH transferred to α-FeOOH and amorphous aluminum hydroxide because of oxidation of Fe(II) in LDH. The second process involved indirect electron transfer from the $Fe^{2+}$ core to the $BrO_3^-$ as shown in Eq. (4):

$$BrO_3^- + 6Fe^{2+} + 6H^+ \rightarrow Br^- + 3H_2O + 6Fe^{3+} \quad (4)$$

Based on the discussion above, the possible mechanism for bromate removal by Fe–Al LDHs seems to take place following two different processes: anion exchange adsorption and reduction. Firstly,

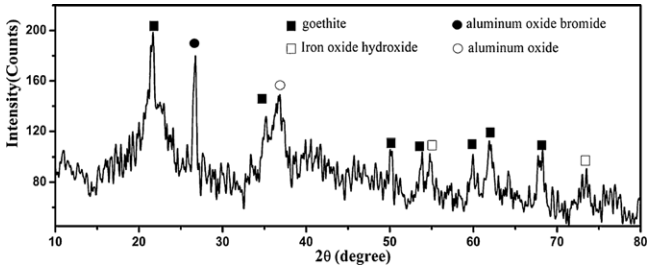


**Fig. 8.** XRD patterns of Fe–Al (30 min) after reaction with bromate.

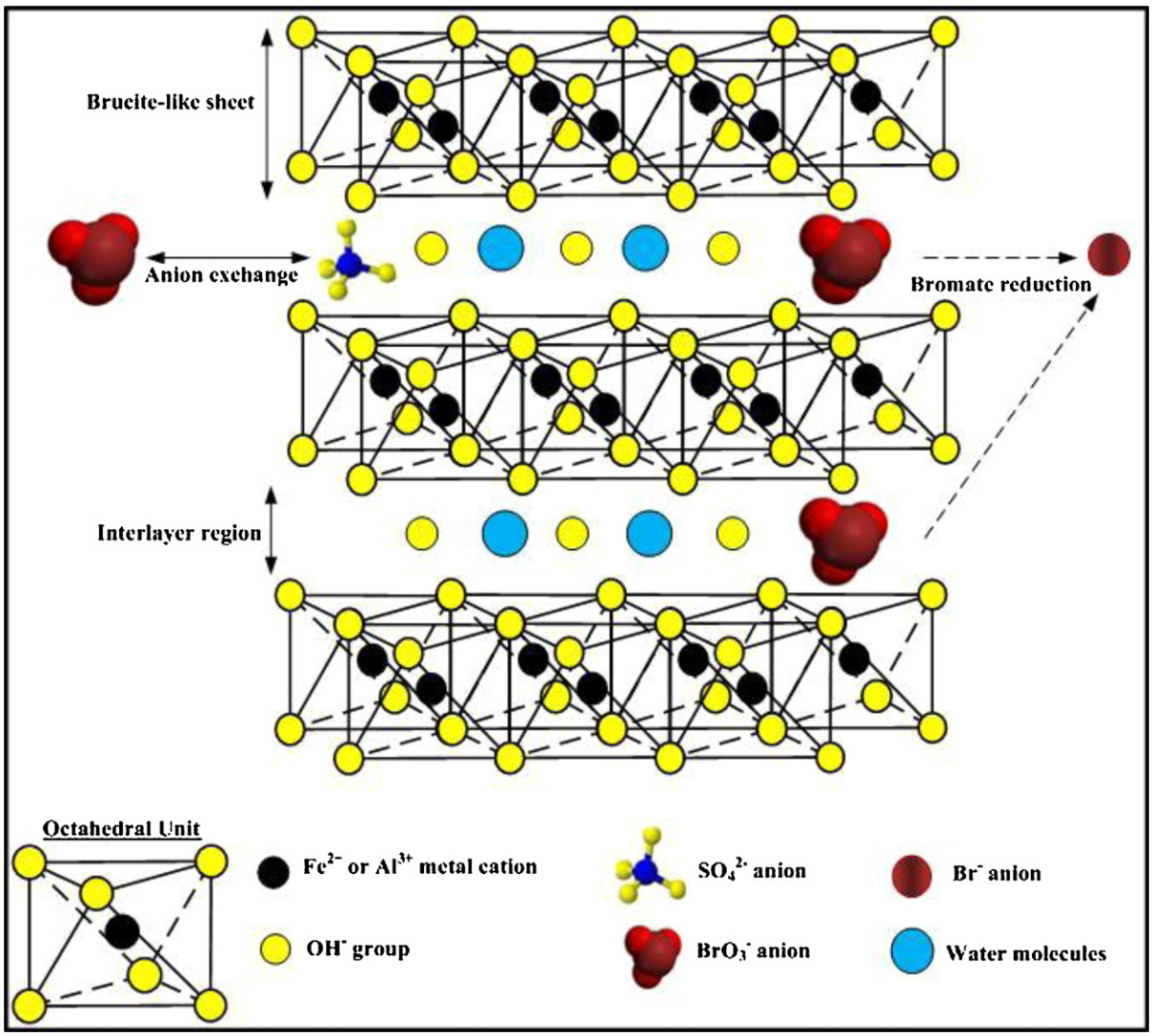


**Fig. 9.** Schematic representation of bromate removal by Fe–Al LDHs.

bromate in solution was absorbed quickly onto the Fe–Al LDHs by ion exchange between sulfate and bromate. Then, the adsorbed bromate was reduced by $Fe^{2+}$ and the innocuous reduced products, bromide, entered into the solution.

A schematic view of the Fe–Al LDHs resembles that of iron(II-III) hydroxysulphate [36], and the schematic view of bromate removal mechanisms by Fe–Al LDHs was illustrated in Fig. 9. Considering that the structure of Fe–Al LDHs could be described as a rhombohedral symmetry (3R) stacking sequence, and the basic structure of Fe–Al LDHs is derived by octahedral unit [28]. The connection between brucite-like sheets and interlayers was realized by hydrogen bonds between the hydrogen atoms of the hydroxyl groups and oxygen atoms of the sulfate groups [36]. Some hydrogen bonded water molecules may occupy the free space in this interlayer region. Various authors have reported sulfate intercalated LDHs or pyroaurite, with the XRD patterns indicating a usual single-plane interlayer [35].

### 3.5. Effect of coexisting anions on bromate removal

The influence of coexisting anions such as chloride ($Cl^-$), sulfate ($SO_4^{2-}$) and phosphate ($PO_4^{3-}$) on bromate removal by Fe–Al LDHs was investigated. The bromate concentration was fixed at 1.56 μmol/L and the initial concentration of coexisting anions varied from 0 to 120 μmol/L. Experimental results indicated that coexisting anions with lower concentration (<36 μmol/L) showed less effect on the bromate removal capacity of Fe–Al LDHs in Fig. S2 (see Supporting information). With the concentration of coexisting anions in solution increasing further, the capacity of bromate removal got worse. The effect of coexisting anions on removal capacity of bromate decreased with the following order: $PO_4^{3-} > SO_4^{2-} > Cl^-$. This order was similar to the Z/r (charge/radius) values of anions: $PO_4^{3-}$ (3/3.40) > $SO_4^{2-}$ (2/2.40) > $Cl^-$ (1/1.81), which suggested that Fe–Al LDHs had stronger affinity toward high valence anions for their higher charge density [44]. As discussed above, the bromate removal by Fe–Al LDHs seems to take place following two different processes: anion exchange adsorption and reduction. The performance of Fe–Al LDHs for bromate adsorption was strongly related to their capability of bromate reduction. Therefore, coexisting anions would compete with bromate for the reactive sites of Fe–Al LDHs and consequently suppress the bromate reduction.

### 3.6. Reuse and stability of Fe–Al LDHs

The reuse of Fe–Al LDHs were investigated in 1.56 μmol/L bromate solution at a solid-to-solution ratio of 1.0 g/L (Fig. S3, see Supporting information). The bromate reduction efficiency of Fe–Al

(30 min) was 100% for the first run. Then the Fe–Al LDHs was separated by filtration, subsequently washed with ultrapure water and finally dried in a vacuum. Three more experiments were repeated using the same materials. The reduction efficiencies of bromate decreased to 65%, 41% and 10% for runs 2, 3 and 4, respectively.

To investigate the stability of the Fe–Al LDHs, the Fe–Al (30 min) stored for 1, 15, 30, and 60 days mixed with 1.56 μmol/L bromate solution at equilibrium pH 7.0, respectively. It was found that bromate was nearly completely reduced to bromide by Fe–Al (30 min) stored 1 and 15 days, indicating that Fe–Al (30 min) was stable up to 15 days after synthesis. Subsequently, the reduction efficiency of bromate decreased from 100% to 85% after 30 days. It further decreased to 66% after 60 days.

The decrease of bromate reduction efficiency in the reuse and stability of Fe–Al LDHs should be attributed to the partial oxidation of $Fe^{2+}$ to $Fe^{3+}$ in LDHs structure [26]. Similar phenomena were also observed in reduction of Cr(VI) and nitrite by green rust [21,45].

## 4. Conclusions

In this study, the Fe–Al LDHs synthesized by the ultrasound-assisted co-precipitation method were used to remove bromate from solution. The ultrasound irradiation was found to be a simple and fast method to assist the preparation of Fe–Al LDHs. When the irradiation time increased from 0 to 30 min, the removal efficiency of bromate by Fe–Al LDHs was increased. The bromate removal was pH independent in the range 7.0–11.0. When the initial bromate concentration was 7.81 μmol/L, the $q_e$ for Fe–Al (0 min) and Fe–Al (30 min) was 6.08 μmol/g and 6.80 μmol/g, respectively. Measured data in the kinetic tests were well described by the pseudo-first-order kinetic model. The mechanism for bromate removal by Fe–Al LDHs involved in the ion-exchange between sulfate and bromate, and the reduction of bromate to bromide by $Fe^{2+}$. Reuse experiments proved that the Fe–Al LDHs could be reused at least four times. In conclusion, Fe–Al LDHs showed great potential in the application of treating bromate-contaminated water.

## Acknowledgements

This research was financially supported by the project of National Natural Science Foundation of China (No. 51078128), International Science & Technology Cooperation Program of China (Nos. 2011DFA90740 and 2012DFB30030-03) and Shanghai Tongji Gao Tingyao Environmental Science & Technology Development Foundation (STGEF).

## Appendix A. Supplementary data

Supplementary data associated with this article can be found, in the online version, at http://dx.doi.org/10.1016/j.jhazmat.2013.01.081.

## References

[1] M. Chairez, A. Luna-Velasco, J.A. Field, X. Ju, R. Sierra-Alvarez, Reduction of bromate by biogenic sulfide produced during microbial sulfur disproportionation, Biodegradation 21 (2009) 235–244.
[2] H.S. Weinberg, C.A. Delcomyn, V. Unnam, Bromate in chlorinated drinking waters: occurrence and implications for future regulation, Environ. Sci. Technol. 37 (2003) 3104–3110.
[3] S.W. Krasner, W.H. Glaze, H.S. Weinberg, P.A. Daniel, I.N. Najm, Formation and control of bromate during ozonation of waters containing bromide, J. Am. Water Works Assoc. 85 (1993) 73–81.
[4] R. Butler, A. Godley, L. Lytton, E. Cartmell, Bromate environmental contamination: review of impact and possible treatment, Environ. Sci. Technol. 35 (2005) 193–217.
[5] X. Zhang, D. De Silva, B. Sun, J. Fisher, R.J. Bull, J.A. Cotruvo, B.S. Cummings, Cellular and molecular mechanisms of bromate-induced cytotoxicity in human and rat kidney cells, Toxicology 269 (2010) 13–23.
[6] T. Umemura, Y. Kurokawa, Etiology of bromate-induced cancer and possible modes of action-studies in Japan, Toxicology 221 (2006) 154–157.
[7] M.M. Moore, T. Chen, Mutagenicity of bromate: Implications for cancer risk assessment, Toxicology 221 (2006) 190–196.
[8] C. Xu, J. Shi, W. Zhou, B. Gao, Q. Yue, X. Wang, Bromate removal from aqueous solutions by nano crystalline akaganeite (β-FeOOH)-coated quartz sand (CACQS), Chem. Eng. J. 187 (2012) 63–68.
[9] M.O. Buffle, S. Galli, U. Von Gunten, Enhanced bromate control during ozonation: the chlorine-ammonia process, Environ. Sci. Technol. 38 (2004) 5187–5195.
[10] E.C. Wert, J.J. Neemann, D. Johnson, D. Rexing, R. Zegers, Pilot-scale and full-scale evaluation of the chlorine-ammonia process for bromate control during ozonation, Ozone-Sci. Eng. 29 (2007) 363–372.
[11] A.H. Konsowa, Bromate removal from water using granular activated carbon in a batch recycle, Desalin. Water Treat. 12 (2009) 375–381.
[12] M.J. Kirisits, V.L. Snoeyink, J.C. Kruithof, The reduction of bromate by granular activated carbon, Water Res. 34 (2000) 4250–4260.
[13] C.T. Matos, S. Velizarov, M.A.M. Reis, J.G. Crespo, Removal of bromate from drinking water using the ion exchange membrane bioreactor concept, Environ. Sci. Technol. 42 (2008) 7702–7708.
[14] N. Kishimoto, N. Matsuda, Bromate ion removal by electrochemical reduction using an activated carbon felt electrode, Environ. Sci. Technol. 43 (2009) 2054–2059.
[15] Q. Wang, S. Snyder, J. Kim, H. Choi, Aqueous ethanol modified nanoscale zerovalent iron in bromate reduction: synthesis, characterization, and reactivity, Environ. Sci. Technol. 43 (2009) 3292–3299.
[16] A. Bhatnagar, Y. Choi, Y. Yoon, Y. Shin, B. Jeon, J. Kang, Bromate removal from water by granular ferric hydroxide (GFH), J. Hazard. Mater. 170 (2009) 134–140.
[17] H. Chen, Z. Xu, H. Wan, J. Zheng, D. Yin, S. Zheng, Aqueous bromate reduction by catalytic hydrogenation over $Pd/Al_2O_3$ catalysts, Appl. Catal. B-Environ. 96 (2010) 307–313.
[18] J. Liu, J. Yu, D. Li, Y. Zhang, M. Yang, Reduction of bromate in a biological activated carbon filter under high bulk dissolved oxygen conditions and characterization of bromate-reducing isolates, Biochem. Eng. J. 65 (2012) 44–50.
[19] R. Chitrakar, A. Sonoda, Y. Makita, T. Hirotsu, Calcined Mg–Al layered double hydroxides for uptake of trace levels of bromate from aqueous solution, Ind. Eng. Chem. Res. 50 (2011) 9280–9285.
[20] K.H. Goh, T.T. Lim, A. Banas, Z. Dong, Sorption characteristics and mechanisms of oxyanions and oxyhalides having different molecular properties on Mg/Al layered double hydroxide nanoparticles, J. Hazard. Mater. 179 (2010) 818–827.
[21] H.C.B. Hansen, O.K. Borggaard, J. Sørensen, Evaluation of the free energy of formation of Fe (II)–Fe (III) hydroxide-sulphate (green rust) and its reduction of nitrite, Geochim. Cosmochim. Acta 58 (1994) 2599–2608.
[22] K.M. Parida, L. Mohapatra, Carbonate intercalated Zn/Fe layered double hydroxide: a novel photocatalyst for the enhanced photo degradation of azo dyes, Chem. Eng. J. 179 (2012) 131–139.
[23] J. Zhang, Y. Li, J. Zhou, D. Chen, G. Qian, Chromium, (VI) and zinc (II) waste water co-treatment by forming layered double hydroxides: mechanism discussion via two different processes and application in real plating water, J. Hazard. Mater. 205–206 (2012) 111–117.
[24] J. Dodds, F. Espitalier, O. Louisnard, R. Grossier, R. David, M. Hassoun, F. Baillon, C. Gatumel, N. Lyczko, The effect of ultrasound on crystallisation-precipitation processes: some examples and a new segregation model, Part. Part. Syst. Char. 24 (2007) 18–28.
[25] Q. Chang, L. Zhu, Z. Luo, M. Lei, S. Zhang, H. Tang, Sono-assisted preparation of magnetic magnesium–aluminum layered double hydroxides and their application for removing fluoride, Ultrason. Sonochem. 18 (2011) 553–561.
[26] R. Chitrakar, Y. Makita, A. Sonoda, T. Hirotsu, Fe–Al layered double hydroxides in bromate reduction: synthesis and reactivity, J. Colloid Interface Sci. 354 (2011) 798–803.
[27] D. Evans, R. Slade, Structural aspects of layered double hydroxides, Struct. Bond. 119 (2006) 1–87.
[28] K. Goh, T. Lim, Z. Dong, Application of layered double hydroxides for removal of oxyanions: a review, Water Res. 42 (2008) 1343–1368.
[29] D.J. Walton, S.S. Phull, Sonoelectrochemistry, in: T.J. Mason (Ed.), Advances in sonochemistry, vol. 4, Jai Press Inc., London, 1996, pp. 205–284.
[30] S.D. Hyman, T.J.W. Lazio, N.E. Kassim, P.S. Ray, C.B. Markwardt, F. Yusef-Zadeh, A powerful bursting radio source towards the Galactic Centre, Nature 434 (2005) 50–52.
[31] Z. Liu, R. Ma, Y. Ebina, N. Iyi, K. Takada, T. Sasaki, General synthesis and delamination of highly crystalline transition-metal-bearing layered double hydroxides, Langmuir 23 (2007) 861–867.
[32] A.R. Abbasi, H. Kalantary, M. Yousefi, A. Ramazani, A. Morsali, Synthesis and characterization of Ag nanoparticles@polyethylene fibers under ultrasound irradiation, Ultrason. Sonochem. 19 (2012) 853–857.
[33] H. Zhang, X. Wen, Y. Wang, Synthesis and characterization of sulfate and dodecylbenzenesulfonate intercalated zinc-iron layered double hydroxides by one-step coprecipitation route, J. Solid State Chem. 180 (2007) 1636–1647.
[34] F. Jiao, X. Chen, L. Liu, Z. Hu, Y. Hu, Y. Wang, Preparation and characterization of Mg–Al/Zn–Al layered double hydroxides intercalated with (+)-2,3-di(p-toluyl)-tartaric acid, J. Mol. Struct. 964 (2010) 152–157.
[35] R. Chitrakar, A. Sonoda, Y. Makita, T. Hirotsu, Synthesis and bromate reduction of sulfate intercalated Fe(II)–Al(III) layered double hydroxides, Sep. Purif. Technol. 80 (2011) 652–657.

[36] L. Simon, M. François, P. Refait, G. Renaudin, M. Lelaurain, J.-M.R. Génin, Structure of the Fe(II–III) layered double hydroxysulphate green rust two from Rietveld analysis, Solid State Sci. 5 (2003) 327–334.
[37] Y. Yang, N. Gao, W. Chu, Y. Zhang, Y. Ma, Adsorption of perchlorate from aqueous solution by the calcination product of Mg/(Al–Fe) hydrotalcite-like compounds, J. Hazard. Mater. 209–210 (2012) 318–325.
[38] D.P. Das, J. Das, K. Parida, Physicochemical characterization and adsorption behavior of calcined Zn/Al hydrotalcite-like compound (HTlc) towards removal of fluoride from aqueous solution, J.Colloid Interface Sci. 261 (2003) 213–220.
[39] L. Wang, J. Zhang, J. Liu, H. He, M. Yang, J. Yu, Z. Ma, F. Jiang, Removal of bromate ion using powdered activated carbon, J. Environ. Sci. 22 (2010) 1846–1853.
[40] L. Lv, P. Sun, Z. Gu, H. Du, X. Pang, X. Tao, R. Xu, L. Xu, Removal of chloride ion from aqueous solution by ZnAl–$NO_3$ layered double hydroxides as anion-exchanger, J. Hazard. Mater. 161 (2009) 1444–1449.
[41] M.J. Kirisits, V.L. Snoeyink, H. Inan, J.C. Chee-Sanford, L. Raskin, J.C. Brown, Water quality factors affecting bromate reduction in biologically active carbon filters, Water Res. 35 (2001) 891–900.
[42] K.B. Ayala-Luis, N.G.A. Cooper, C.B. Koch, H.C.B. Hansen, Efficient dechlorination of carbon tetrachloride by hydrophobic green rust intercalated with dodecanoate anions, Environ. Sci. Technol. 46 (2012) 3390–3397.
[43] L. Xie, C. Shang, The effects of operational parameters and common anions on the reactivity of zero-valent iron in bromate reduction, Chemosphere 66 (2007) 1652–1659.
[44] L. Lv, J. He, M. Wei, D. Evans, X. Duan, Factors influencing the removal of fluoride from aqueous solution by calcined Mg–Al–$CO_3$ layered double hydroxides, J. Hazard. Mater. 133 (2006) 119–128.
[45] A.G.B. Williams, M.M. Scherer, Kinetics of Cr (VI) reduction by carbonate green rust, Environ. Sci. Technol. 35 (2001) 3488–3494.